Development of electrostatic-induced charge detector for multiturn time-of-flight mass spectrometer

Short title
Development of non-destructive ion detector for multiturn TOF–MS

Ken-ichi Bajo[1 *], Jun Aoki[2, 3, 4], Morio Ishihara[2], Shizuho Furuya[5], Masahiro Nishimura[5], Miwa Yoshitake[5] and Hisayoshi Yurimoto[1, 5]

[1] Department of Earth and Planetary Sciences, Hokkaido University, Sapporo, Japan

[2] Department of Physics, Graduate School of Science, Osaka University, Toyonaka, Japan

[3] Graduate School of Frontier Biosciences, Osaka University, Suita, Japan

[4] Riken Center for Biosystems Dynamics Research, Kobe, Japan

[5] ISAS/JAXA, Sagamihara, Japan

[*] Corresponding author. E-mail: k-bajo@eis.hokudai.ac.jp Tel.: +81 11 706 9174.

Keywords: multiturn TOF–MS, electrostatic-induced charge detector, MULTUM, non-destructive ion detection, mass assignment

Abstract

We developed an autocorrelation function to resolve the overtaking problem in a multiturn time-of-flight mass spectrometer (TOF–MS). The function analyzes the characteristic period for one lap of each ion packet and derives a mass spectrum from a signal pulse train composed of multiturn ion packets. To detect the ion pulse train, a new non-destructive ion detector was developed and installed in the multiturn orbit of MULTUM-S II. This detector is composed of an electrostatically induced charge detector, a preamplifier, and a digitizer. The electrostatic noises are smaller than the single-ion signals owing to the accumulation of the multiturn TOF spectrum. The conventional ion detector of TOF–MS is operated after collecting the signal pulse train. The multiturn TOF spectrum was convolved with an autocorrelation function to derive the mass spectrum. The convolved mass spectrum performed a mass resolving power (MRP) of 28,200 at m/z 69 and mass accuracy of 28 ppm for the perfluorotributylamine (PFTBA) gas sample.

1. Introduction

Multiturn ion optics with perfect space and time focusing were developed to achieve infinite mass resolving power (MRP) time-of-flight mass spectrometry.[1] The optics were installed in time-of-flight mass spectrometers (TOF–MS), MULTUM, and MULTUM II, which provide ultra-high MRP to attain an $M/\Delta M = 6 \times 10^5$.[2-8] The optics also dramatically reduce the size of TOF–MS.

Although the optics provided ultra-high MRP with a compact MS, it introduced the so-called overtaking problem for the mass spectrum, in which ions having small *m/z* overtake ions having large *m/z* when the flight time (pass length) is increased.[9] As a result, the time-of-flight (TOF) spectrum after the flight is not aligned according to *m*/*z*. When many ion species with different *m*/*z* simultaneously fly in the multiturn trajectory, the overtaking ions complicate the TOF spectrum. This characteristic makes the universal use of multiturn TOF–MS difficult, and the applications may be restricted to a narrow range of *m*/*z* in the multiturn trajectory.[10,11] In this study, we traced every multiturn ion using a novel electrostatic-induced charge detector (iCD) installed in multiturn optics. We analyzed the overtaking problem of the multiturn TOF spectrum using an autocorrelation function to derive the mass spectrum.

2. Electrostatic-induced charge detector (iCD)

An electron impact (EI) type TOF–MS, infiTOF (MSI. TOKYO, Inc., Japan), equipped with MULTUM-S II was used.[9, 12] An iCD was installed in the ion optics of the MULTUM-S II (Figure 1a).

A stainless steel tube with an inner diameter of 6 mm and a length of 18 mm was used to make the iCD. The iCD connects the input gate electrode of a field-effect transistor to a charge-sensitive preamplifier (CSA) A250CF CoolFET® (Amptek Inc., USA) (Figure 1b). The iCD is shielded by an exterior body at ground potential. The iCD was set in the multiturn ion optics between the electrostatic sectors of the MULTUM-S II (Figure 1a). The electrostatic-induced charges caused by a multiturn ion packet were detected by the iCD. When an ion packet with positive charges (+Q) passes through the iCD, charges −Q and +Q are induced on the inner and outer surfaces of the iCD, respectively. The +Q charges can be measured using CSA without any effect on the ion packet (Figure 1b). The output voltage is 0.64 μV when a single charged ion passes through the iCD.

3. Data acquisition system

A schematic illustrating the data acquisition system for the electrostatic-induced

charge detection is shown in Figure 2. This system resembles that of the data acquisition system reported by Bajo et al.[13] The pulse signals from the A250CF preamplifier are converted into 10-bits digital signals using the NI PXIe-5160 (5160) digitizer. The sampling rate and voltage resolution are 104.167×10^6 samples s^{-1} and 48.8 μV (10-bits and ± 0.025V for peak-to-peak voltage), respectively. Streaming data processing and recording are performed using the NI PXIe-8880 (8880) as a controller of the PXI-platform (National Instruments corp., USA). This system is controlled using the LabVIEW program.

The 10-bits digital signals are converted into 16-bits iCD spectrum, and then multiplied and subtracted by the gain and the offset of 5160 digitizer settings, respectively. The arbitrary repetitive acquisition data for the iCD spectra are converted into 64-bits double precision floating point numbers and averaged. The acquisition data are stored in the 8880. A master-trigger of 1 V rectangle pulse from the infiTOF is used and introduced to a digital delay/pulse generator (Model 575, Berkeley Nucleonics Corporation, USA). The Model 575 converts to a transistor-transistor-logic pulse from the master-trigger and outputs to the digital multimeter NI PXIe-6361. Trigger synchronization among the converted master-trigger and PXI modules is performed using real-time system integration in the backplane of the NI PXIe-1082 chassis.

The noise characteristics of the iCD system are evaluated by a blank spectrum, which is produced by the same data acquisition procedure as the normal infiTOF operation[9] without the extraction of ions from the EI source. The baseline of the iCD spectrum is modulated by switching pulse noises derived from the rising and falling voltages of the entrance and exit deflection electric sectors of MULTUM-S II (Figure 3). To remove the modulation, a ± 48 ns moving average was applied to the blank iCD spectrum. The moving average was repeated 20 times. The moving average spectrum was subtracted from the blank iCD spectrum. The standard deviations of the noise signals decrease theoretically with increasing accumulation of the blank iCD spectrum with a slope to the power of ~ −0.5 (Figure 4). For an iCD spectrum, the estimated noise signal is 1000 ions, while for iCD spectra obtained after 10^8 accumulations, the estimated noise signal is ~0.3. This indicates that after 10^8 accumulations, single-ion detection with three standard deviation reliability is obtained. Thus, a dynamic range of this system is estimated to $\sim 3 \times 10^4$ because $\sim 10^4$ ions from the ion source can be extracted for single mass scan and the minimum noise level is ~0.3 ion.

4. Experimental method

N_2 and perfluorotributylamine (PFTBA, molecular weight: 671) gases are used.

N_2 gas is introduced into the EI ion source of the infiTOF with He as the carrier gas. In the case of PFTBA, the vaporized gas is directly introduced into the ion source. The pressure in the ionization chamber is set to ~1×10^{-2} Pa during the measurements. The ion packet produced in the ion source is introduced into the ion trajectory of the MULTUM-S II using an entrance electric sector (Figure 1a). The voltage of the entrance electric sector drops to the ground potential before the ions return to the sector. The signals from ion packets during multiturning are detected by the iCD system. After multiturning, the ion packets are output using an exit electric sector and detected by an electron multiplier (EM) (148006 Fast-TOF Plus, ETP Ion Detect Pty Ltd., Australia).

5. Data reduction procedure

5.1. Baseline correction

Figure 5 shows the iCD spectrum of the N_2–He gas mixture measured 2.4×10^6 times and averaged. Random noise levels of the accumulated spectrum correspond to 0.61 μV or 0.95 ions as standard deviation (Figure 4).

The baseline of the iCD spectrum is modulated by the entrance pulses, as discussed in Section 3 (Figure 5). The modulations of the baseline are removed in the following steps: (1) selecting ion signals from the iCD spectrum using a differential filter (Figures $6a_1$, $6a_2$, and 6b). Absolute ion intensities larger than the noise level in Figure 6b are defined as peaks of ion signals. The standard deviation described above (0.95 ions) was used as the noise level. Each peak of ion signals is defined as ± 58 ns outward from the boundary between the peak profile and the noise level. The time width is determined by the peak widths of several high peak profiles. The ion and noise signals are shown in yellow and black, respectively (Figure 6c). (2) Ion signals from the differential iCD spectrum are removed from the iCD spectrum. The removed areas are interpolated linearly between both ends of the remaining data (Figure 6d). (3) To obtain the modulated baseline profile, a ± 48 ns moving average is applied to the interpolated spectrum 20 times (Figure 6e as a baseline profile of Figure $6a_2$). (4) The baseline profile is subtracted from the iCD spectrum (Figures $6f_1$ and $6f_2$). The baseline-corrected iCD spectrum is shown in Figure 7.

5.2. Convolution of iCD mass spectrum with autocorrelation function

An ion packet of m/z periodically passes through the iCD with a lap time of τ. The autocorrelation function shown below converts the baseline-corrected iCD spectrum into a mass spectrum: A function $f(\tau, t)$ that defines the ion packet $C(\tau)$ is denoted as the conditional series sum of $Q(i\tau)$, which is the charge of an ion packet for each lap.

$$f(\tau,\ t) = \sum Q(\tau, t)\, g(\tau, t) = \sum_{i=1}^{n} Q(i\tau, t)\frac{1}{n} \quad (1)$$

where t is a variable of TOF, and i is the multiturn number.

At time $t = t_a$,

$$g(\tau, t) = \begin{cases} 0\ (Q(i\tau, t_a) < -V_{dis}) \\ 1\ (Q(i\tau, t_a) \geq -V_{dis}) \end{cases} \quad (2)$$

where V_{dis}, discrimination voltage between peaks and noise, is based on the noise level of the iCD spectrum. This operation removes noise signals from the iCD spectrum. The standard deviation of the noise of the measurement condition was set at V_{dis} = 0.6 μV. Furthermore, we set Q ((i + 1) τ, t_a) = Q ($i\tau$, t_a) if Q ((i + 1) τ, t_a) is greater than Q ($i\tau$, t_a). This operation removes the contribution of the overlapping ion peaks in the iCD spectrum. Then, $C(\tau)$ can be expressed by the following equation:

$$C(\tau) = \int f(\tau, t)dt \quad (3)$$

Expanding this expression, we get the following equation:

$$C(\tau) = \int_{-\Delta t}^{\Delta t} \frac{1}{n}\{Q(\tau + t_0 + t) + Q(2\tau + t_0 + t) + \cdots + Q(n\tau + t_0 + t)\}dt \quad (4)$$

where t_0 is the TOF of the ion packet from the exit slit of the ion source to the iCD, which is proportional to τ depending on the m/z, i.e., t_0 = 0.3781 τ. The coefficient 0.3781 is a unique constant for the MULTUM-S II. Δt is the value that complements to t_0. We set Δt = 288 ns, which is nearly twice the peak width of the iCD spectrum (Figure 7b). A larger Δt provides a higher redundancy for the calculation but are computationally expensive.

A convolution from the iCD spectrum to the mass spectrum is calculated as $C(\tau)$ over a range of τ_{min} to τ_{max} in s_τ increments. The τ_{min} and τ_{max} are determined from the mass spectrum obtained using MULTUM-S II operated in the half-cycle mode.[9] The s_τ corresponds to the resolution of the m/z axis. We set s_τ = 0.5 ns to derive a mass spectrum of appropriate mass resolution. The m/z is calculated from τ if we use one or more internal mass references.

Figure 8 shows the mass spectrum of the N_2−He gas mixture convolved using Equation (4) from the iCD spectrum, as shown in Figure 7a. The m/z is calculated using the ^{4}He and $^{28}N_2$ signals as internal mass references. The largest ion intensity among the ions is in the mass spectrum with $^{28}N_2^+$ as the sample gas, and the second largest is in the spectrum with $^4He^+$ as the carrier gas. We observed $^{14}N^{15}N^+$ of the N_2 isotopologue and $^{14}N^+$ as fragment ion of N_2. Peaks of $H_2{}^{16}O^+$, $^{32}O_2^+$, and $^{40}Ar^+$ were also detected, which were from the residual air in the ion source.

5.3. Mass resolving power of the convolved mass spectrum

Given an ion packet at i laps of the iCD spectrum, the MRP of the ion packet peak, MRP_{iCD} is calculated as:

$$MRP_{iCD}(i) = \frac{i\tau}{2\Delta T_i} = \frac{iL}{2l_{iCD}} \quad (5)$$

where ΔT_i is the full half-width maximum of the ion peak at i laps, L is the flight pass length for one lap, and l_{iCD} is the length of the iCD tube. The L and l_{iCD} for MULTUM-S II are 0.65 m and 0.018 m, respectively.

According to Equation (5), the MRP_{iCD} of N_2^+ increases linearly with increasing $\underline{i}$ (Figure 9). The MRP of the convolved mass spectrum, MRP_{conv} calculated from Figure 8 also increases linearly with increasing $\underline{i}$, but the slope is one-third of the slope of MRP_{iCD} because of averaging the iCD N_2 peaks. This indicates that the MRP performance improves if we combine the convolved mass spectrum and ion peaks extracted from the iCD spectrum.

6. Extended convolution using iCD and multiturn TOF spectra (Extended convolved mass spectrum)

To overcome the lower MRP performance of the convolved mass spectrum, we applied a combination analysis between the iCD and the conventional EM ion detector. Therefore, we used the experimental results of PFTBA because the characteristics of the mass spectrum of PFTBA have been well studied and widely used for the mass calibration of EI mass spectrometry.[14]

The multiturn TOF spectrum of PFTBA measured using the EM detector is shown in Figure 10. The convolved mass spectrum calculated from the simultaneously measured iCD spectrum is shown in Figure 11. In this calculation, we set $V_{\mathrm{dis}} = 0$ V instead of 0.6 μV to reject small ion signals close to noises.

We combined the convolved mass spectrum and multiturn TOF spectrum to formulate an extended convolved mass spectrum. To replace the peaks of the convolved mass spectrum with the peaks of the multiturn TOF spectrum, Equation (4) is changed to:

$$C(t) = I_{EM}(n\tau + t_0 + t_{ex}) \quad (6)$$

where I_{EM} is the ion intensity of the multiturn TOF spectrum at $(n\tau + t_0 + t_{\mathrm{ex}})$. t_{ex} is the TOF from the iCD to the EM detector to extract from the multiturn trajectory and is given as:

$$t_{ex}(m/z) = t_a(m/z)^{1/2} + t_b \quad (7)$$

where t_{a} and t_{b} are constants given by the MS conditions (acceleration, toroidal sector electric fields, and MATSUDA plate voltages). In this study, we determined t_{a} and t_{b} using internal mass references at m/z 68.9952 (CF_3^+) and 218.9856 ($C_4F_9^+$). Using Equation (6),

we replaced the peaks appearing in Figure 11 with those appearing in Figure 10 to construct an extended convolved mass spectrum of PFTBA (Figure 12). We compared the peaks at *m/z* 130.9920 ($C_3F_5^+$) in the mass spectra (Figure 13). The MRP of the extended convolved mass spectrum is the fully performed multiturn ion trajectory of the MULTUM-S II.

The TOF of a peak of ion x on the multiturn TOF spectrum, T_x is expressed as:

$$T_x = \frac{n_x L + l}{v_x} \tag{8}$$

where n_x is the number of multiturn laps of ion x at extraction, l is the flight pass length for half-cycle mode operation, and v_x is the flight speed of ion x. The flight pass lengths are independent of ion x. From the peaks of ions x and y, we get:

$$\frac{v_x}{v_y} = \sqrt{\frac{m_y}{m_x}} \tag{9}$$

where m_i and m_j are the masses of the ions x and y, respectively. Then, L and l are expressed as:

$$L = \frac{T_x v_x - T_y v_y}{n_x - n_y} = \frac{T_x - T_y\sqrt{\frac{m_x}{m_y}}}{n_x - n_y}\, v_x = \tau_x v_x \tag{10}$$

$$l = v_x(T_x - n_x\tau_x) \tag{11}$$

where τ_x is the lap time of ion x. Therefore, if ions x and y are used as internal references, the T_z for ion z is calculated as:

$$T_z = (\tau_x(n_z - n_x) + T_x)\sqrt{\frac{m_z}{m_x}} \tag{12}$$

$$m_z = m_x T_z^2 (\tau_x(n_z - n_x) + T_x)^{-2}. \tag{13}$$

The measured masses m_z on the extended convolved mass spectrum were calculated from Equation (13) using two internal mass reference peaks of CF_3^+ and $C_4F_9^+$. The molecular formulas, exact masses, measured masses, mass differences, mass accuracies, number of laps, and MRPs for PFTBA fragment ions are summarized in Table 1. The mass accuracies are less than 80 ppm. The root mean square of the mass accuracies of the system is 28 ppm. The value 28 ppm corresponds to the modulation amplitude of the power supply because modulation causes fractionations of the lap time of ions by voltage modulations of the electric sectors.[8]

7. Conclusions

We developed an iCD system to obtain mass spectra in a non-destructive mode. We also formulated an autocorrelation function for this system to resolve the overtaking problem in the multiturn TOF–MS. The iCD system provides *m/z* assignments of flying

ions along the multiturn trajectory. A mass spectrum was constructed from the iCD spectra. An MRP of up to ~30,000 and mass accuracy of tens of ppm have been realized by the iCD system installed in the MSI infiTOF.

227 Acknowledgements
228 We thank the anonymous reviewer for the constructive comments. We would
229 like to thank Editage (www.editage.com) for English language editing.

References

1. Ishihara M, Toyoda M, Matsuo T. Perfect space and time focusing ion optics for multiturn time of flight mass spectrometers. *Int J Mass Spectrom.* 2000;197(1-3):179-189. doi.org/10.1016/S1387-3806(99)00244-4
2. Matsuo T, Ishihara M, Toyoda M, Ito H, Yamaguchi S, Roll R, Rosenbauer H. A space time-of-flight mass spectrometer for exobiologically-oriented applications. *Adv Space Res.,* 1999;23(2):341-348. doi.org/10.1016/S0273-1177(99)00055-1
3. Toyoda M, Ishihara M, Yamaguchi S, Ito H, Matsuo T, Roll R, Rosenbauer H. Construction of a New Multi-turn Time-of-Flight Mass Spectrometer. *J Mass Spectrom*. 2000;35(2):163-167. DOI: 10.1002/(SICI)1096-9888(200002)35:2<163::AID-JMS924>3.0.CO;2-G
4. Toyoda M, Okumura D, Yamaguchi S, Ishihara M, Katakuse I, Matsuo T. Development of a multi-turn time-of-flight mass spectrometer 'MULTUM Linear plus'. *J Mass Spectrom Soc Jpn.* 2000;48(5):312-317. doi.org/10.5702/massspec.48.312
5. Toyoda M, Okumura D, Ishihara M, Katakuse I. Multi-turn time-of-flight mass spectrometers with electrostatic sectors. *J Mass Spectrom.* 2003;38(11):1125-1142. doi.org/10.1002/jms.546
6. Okumura D, Toyoda M, Ishihara M, Katakuse I. A simple multi-turn time of flight mass spectrometer 'MULTUM II'. *J Mass Spectrom Soc Jpn.* 2003;51(2):349-353. doi.org/10.5702/massspec.51.349
7. Okumura D, Toyoda M, Ishihara M, Katakuse I. Application of a multi-turn time-of-flight massspectrometer, MULTUM II, to organic compounds ionized by matrix-assisted laser desorption/ionization. *J Mass Spectrom.* 2004;39(1):86-90, 2004. DOI: 10.1002/jms.575
8. Tonotani A, Bajo K, Itose S, Ishihara M, Uchino K, Yurimoto H. Evaluation of multi-turn time-of-flight mass spectrum of laser ionization mass nanoscope. *Surf Interface Anal*. 2016;48(11):1122-1126. doi.org/10.1002/sia.6112
9. Shimma S, Nagao H, Aoki J, Takahashi K, Miki S, Toyoda M. Miniaturized high-resolution time-of-flight mass spectrometer MULTUM-S II with an infinite flight path. *Anal Chem.* 2010;82(20), 8456-8463, 2010. doi.org/10.1021/ac1010348
10. Shimma S, Nagao H, Giannakopulos AE, Hayakawa S, Awazu K, Toyoda M. High-energy collision-induced dissociation of phosphopeptides using a multi-turn tandem time-of-flight mass spectrometer 'MULTUM-TOF/TOF'. *J Mass Spectrom*. 2008;43(4):535-537. DOI: 10.1002/jms.1352
11. Shimma S, Miki S, Toyoda M. Polychlorinated biphenyls (PCBs) analysis using a

miniaturized high-resolution time-of-flight mass spectrometer "MULTUM-S II". *J Environ Monit*. 2012;14(6):1664-1670. doi.org/10.1039/C2EM30112A

12. Shimma S, and Toyoda M. In *Greenhouse Gases - Emission, Measurement and Management*, (Ed: G. Liu) 2012; Intech Open, London. pp. 235–254. doi: 10.5772/33815
13. Bajo K, Fujioka O, Itose S, Ishihara M, Uchino K, Yurimoto H. Electronic data acquisition and operational control system for time-of-flight sputtered neutral mass spectrometer. *Surf Interface Anal.* 2019; 51(1): 35-39. doi.org/10.1002/sia.6541
14. NIST Standard Reference Database 69: NIST Chemistry WebBook, https://doi.org/10.18434/T4D303

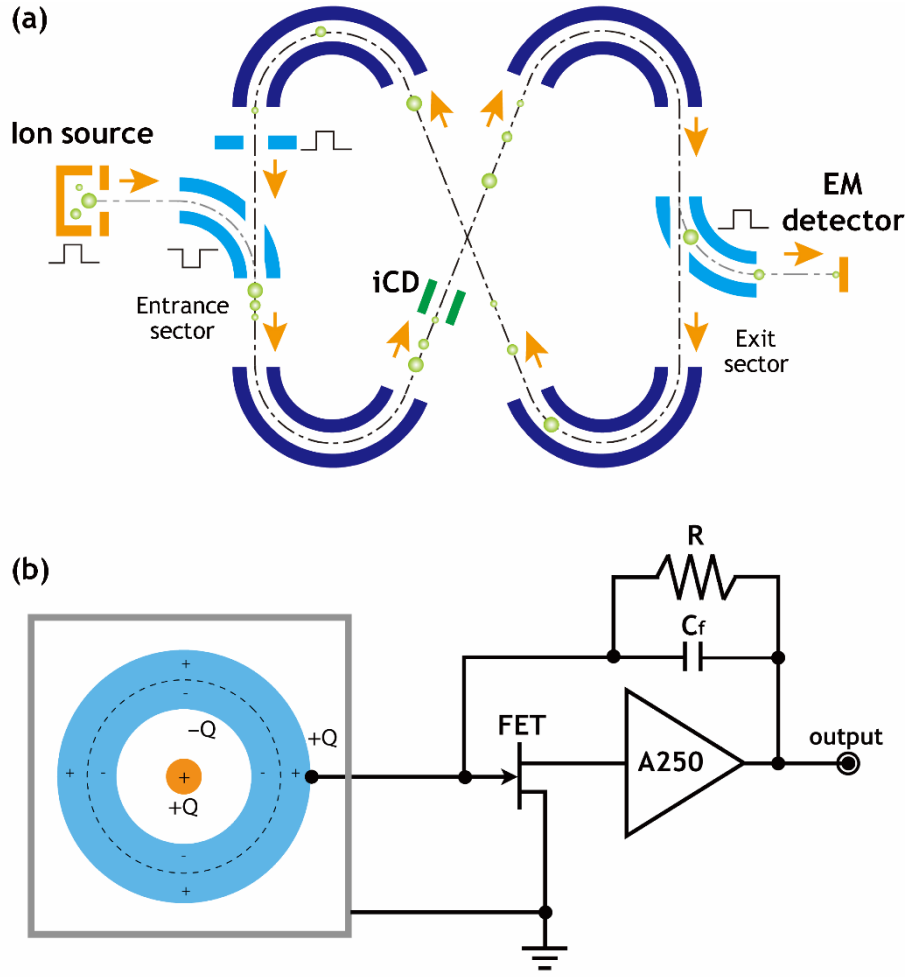

Figure 1. (a) Schematic of electrostatic-induced charge detector (iCD) installed in MULTUM-S II and ion detection using a secondary EM detector (b) Schematic of charge readout for ion packet charged +Q.

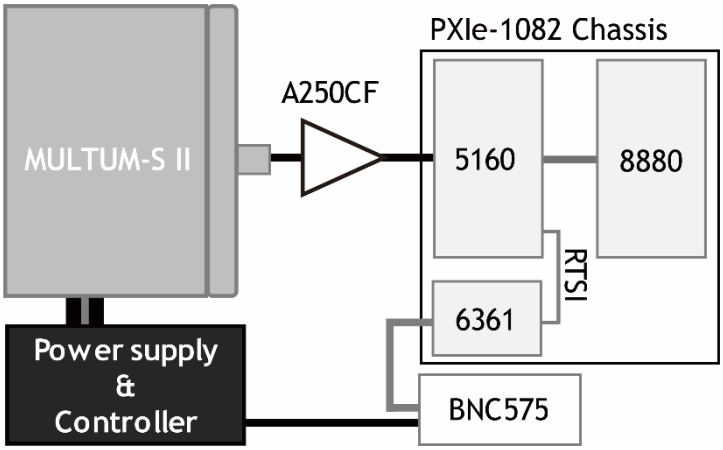

Figure 2. Schematic of data acquisition system for iCD. Outputs from A250CF preamplifier are converted to 10-bits digital signals using PXIe-5160 (5160) digitizer. The digital signals are processed and stored by PXIe-8880 (8880). BNC575 and PXIe-6361(6361) controls timing for data acquisition.

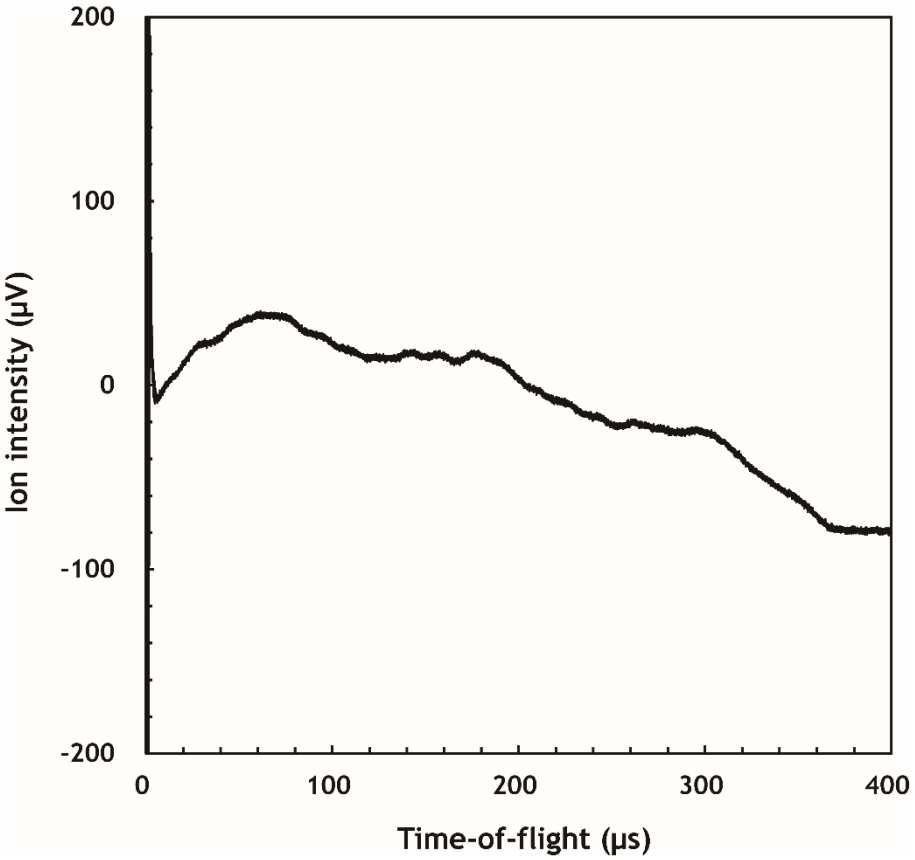

Figure 3. Baseline of an iCD spectrum, of which accumulation of the iCD spectra was 2.4×10^6.

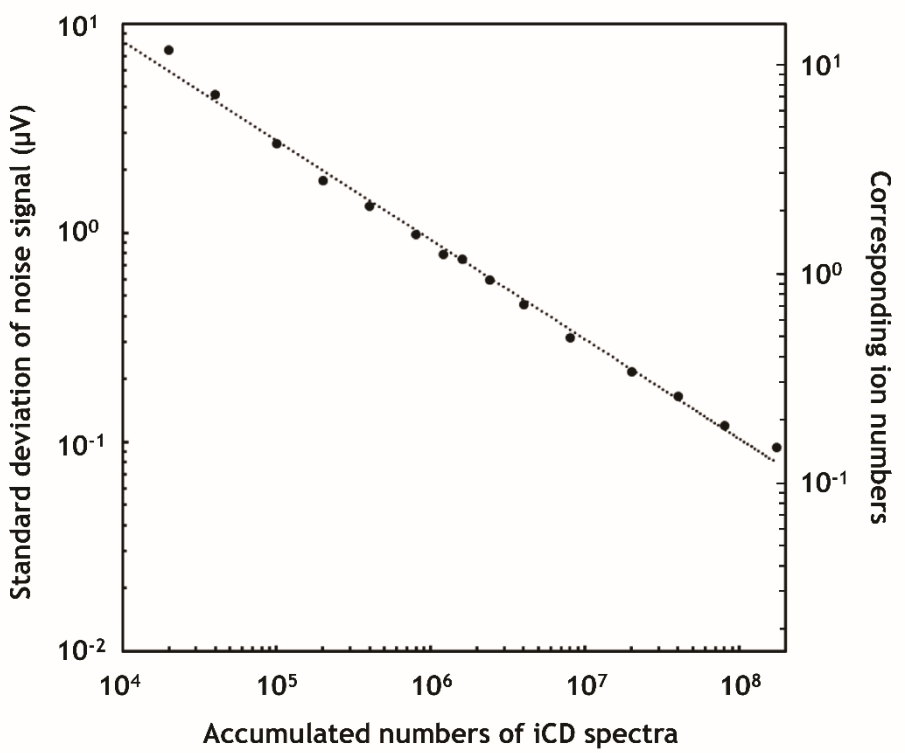

Figure 4. Standard deviations of noise signal as a function of accumulated numbers of iCD spectra. Dotted line represents a power approximate expression (y (μV) = 664.0 $x^{-0.476}$).

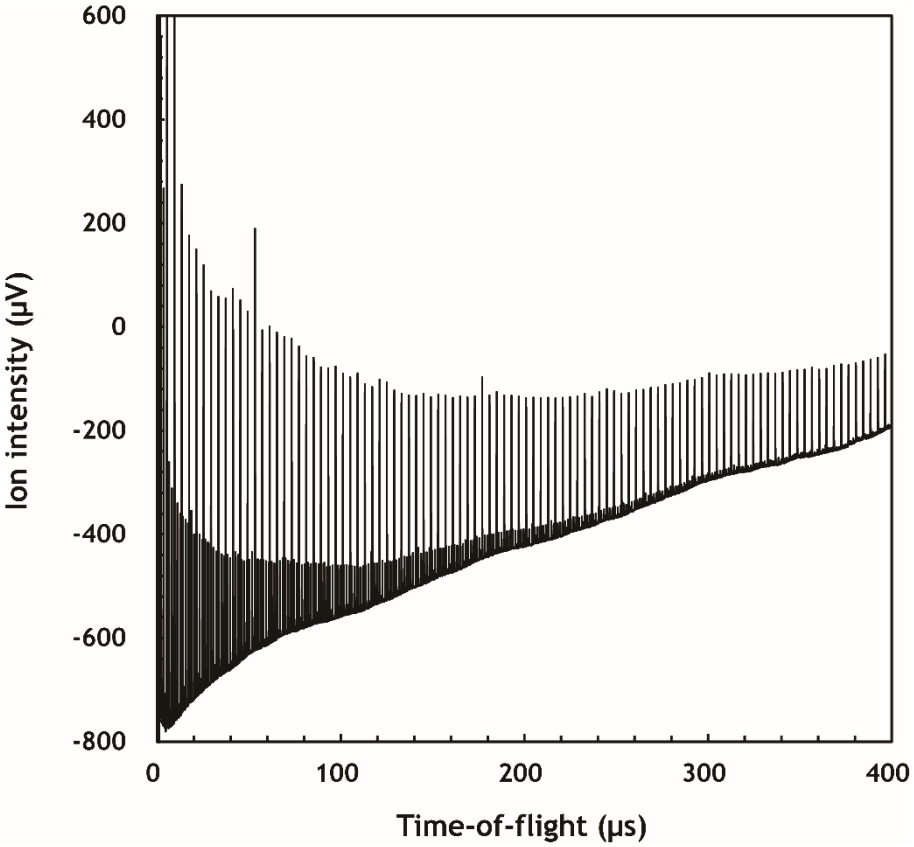

Figure 5. iCD spectrum of N_2–He gas.

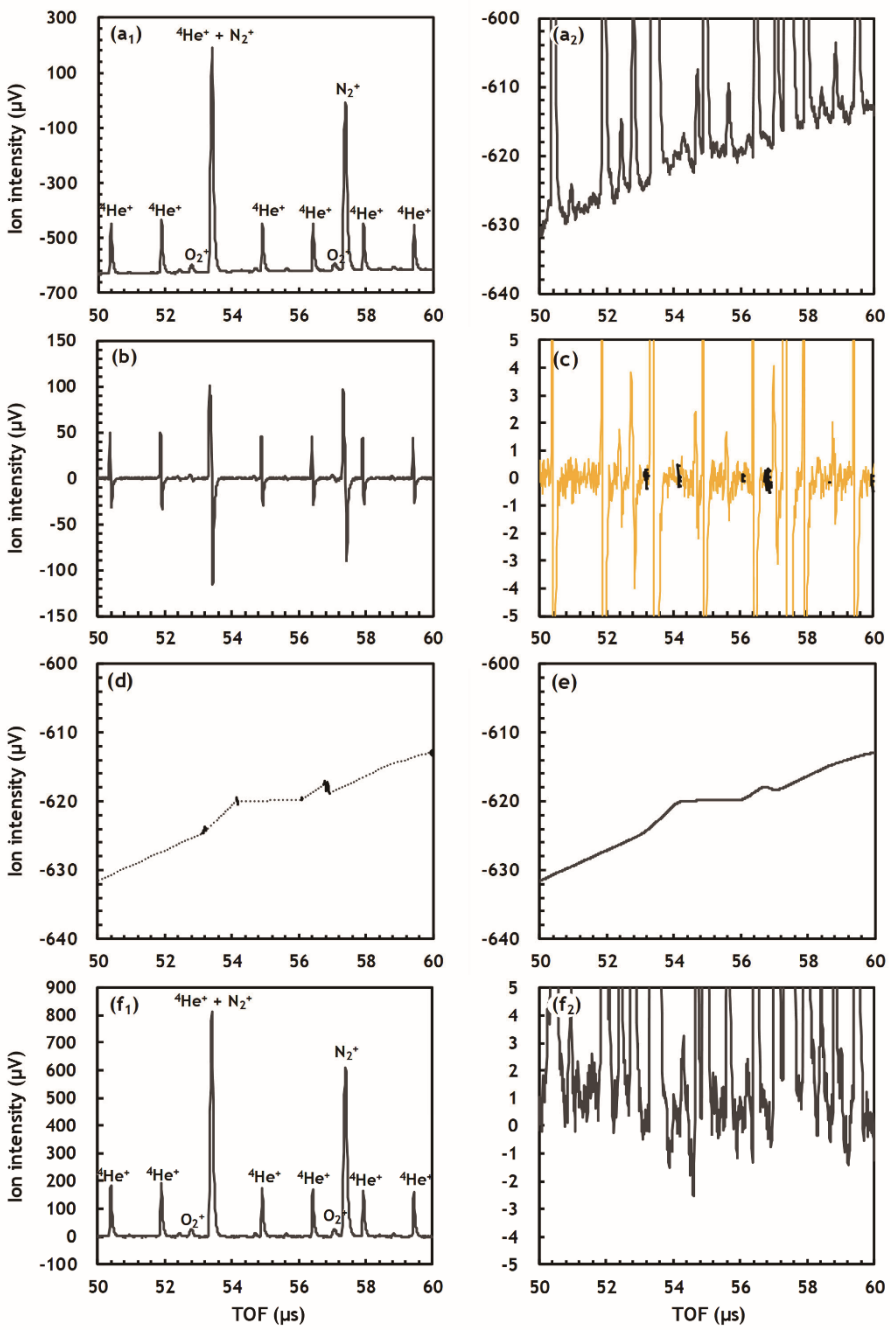

Figure 6. Procedure of baseline correction. (a_1) An enlarged iCD spectrum of Figure 5 (50 μs to 60 μs). (a_2) An enlarged iCD spectrum of the baseline of (a_1). (b) A differential iCD spectrum of (a_1). (c) An enlarged differential iCD spectrum of (b). Ion and noise signals are shown in yellow and black, respectively. (d) The noise signals of (c) are removed and interpolated linearly (dotted line). (e) Smooth profile of (d) as modulated baseline profile of (a_2). (f_1) A baseline-corrected iCD spectrum. Full spectrum is shown in Figure 7. (f_2) An enlarged baseline-corrected iCD spectrum of (f_1).

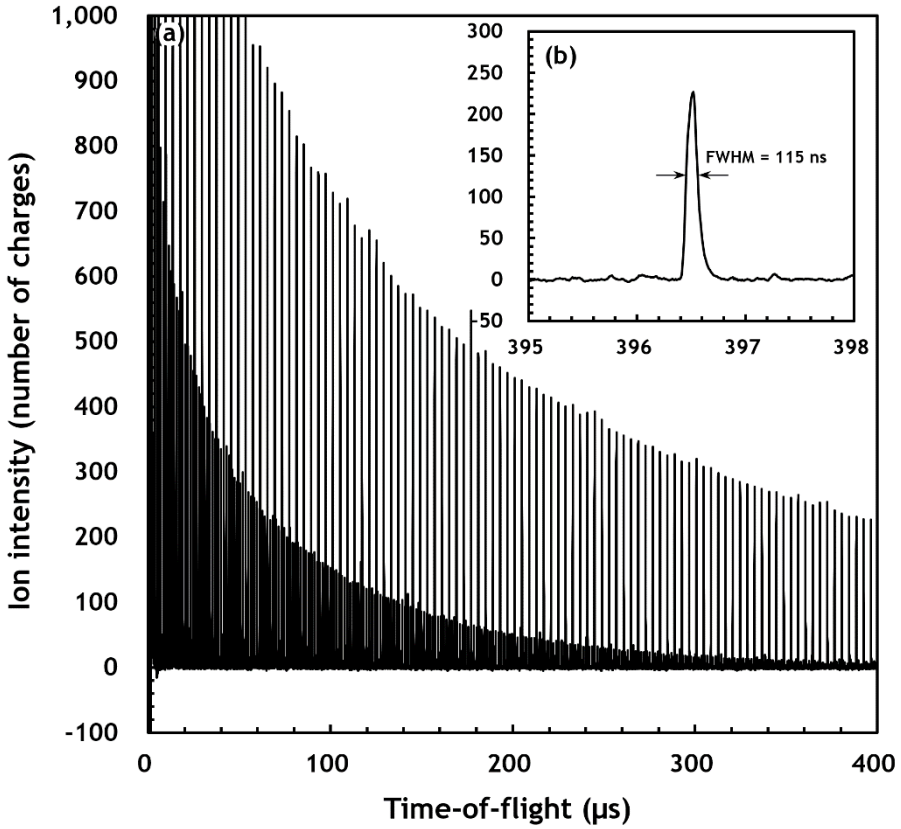

Figure 7. (a) Baseline-corrected iCD spectrum of N_2–He gas. (b) A spectrum at 396.5 μs.

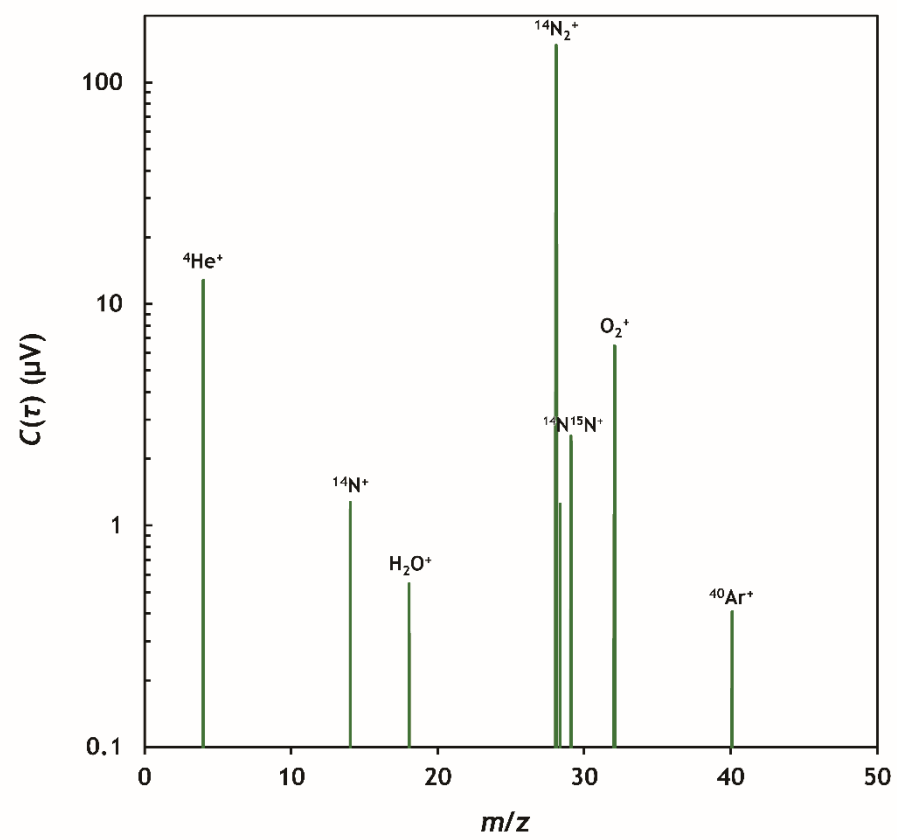

Figure 8. Convolved mass spectrum of N_2–He gas calculated from iCD spectrum. τ_{min}, τ_{max}, $s_{\tau,}$ $t_{0,}$ Δt and V_{dis} were set at 0.96 μs, 4.80 μs, 0.5 ns, 0.3781 τ, 288 ns, and 0.6 μV, respectively. The *m/z* (horizontal axis) is calculated from τ using internal mass references at *m/z* 4.00260 ($^4He^+$) and 28.00615 ($^{28}N_2^+$).

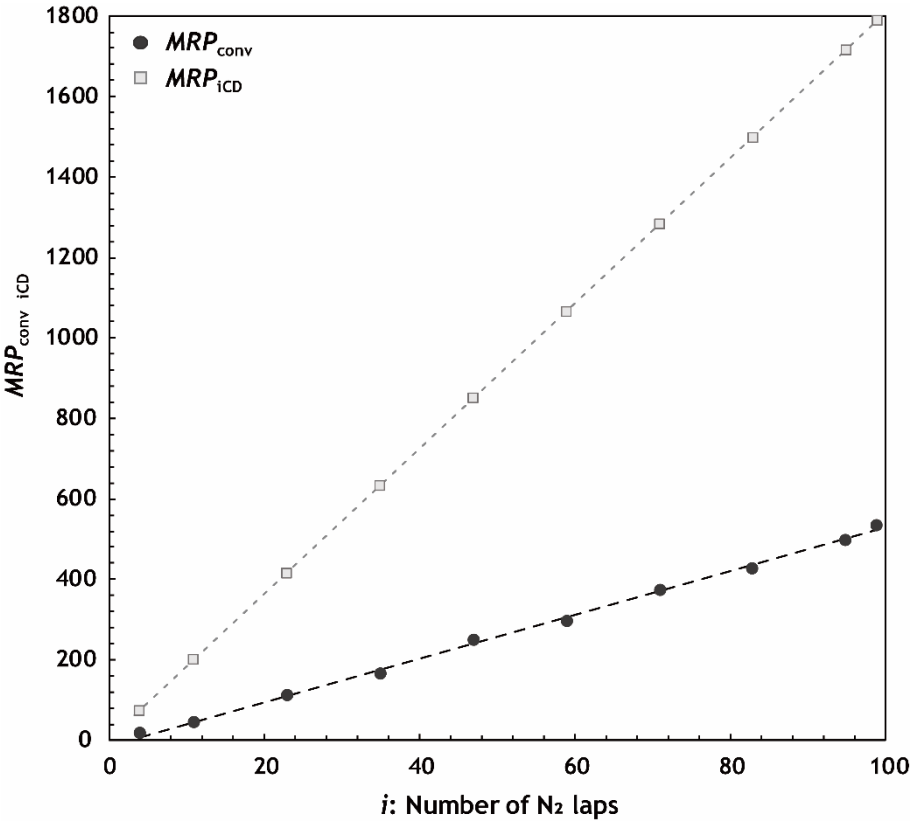

Figure 9. Change of MRP_{conv} and MRP_{iCD} of N_2^+ as a function of number of multiturn laps.

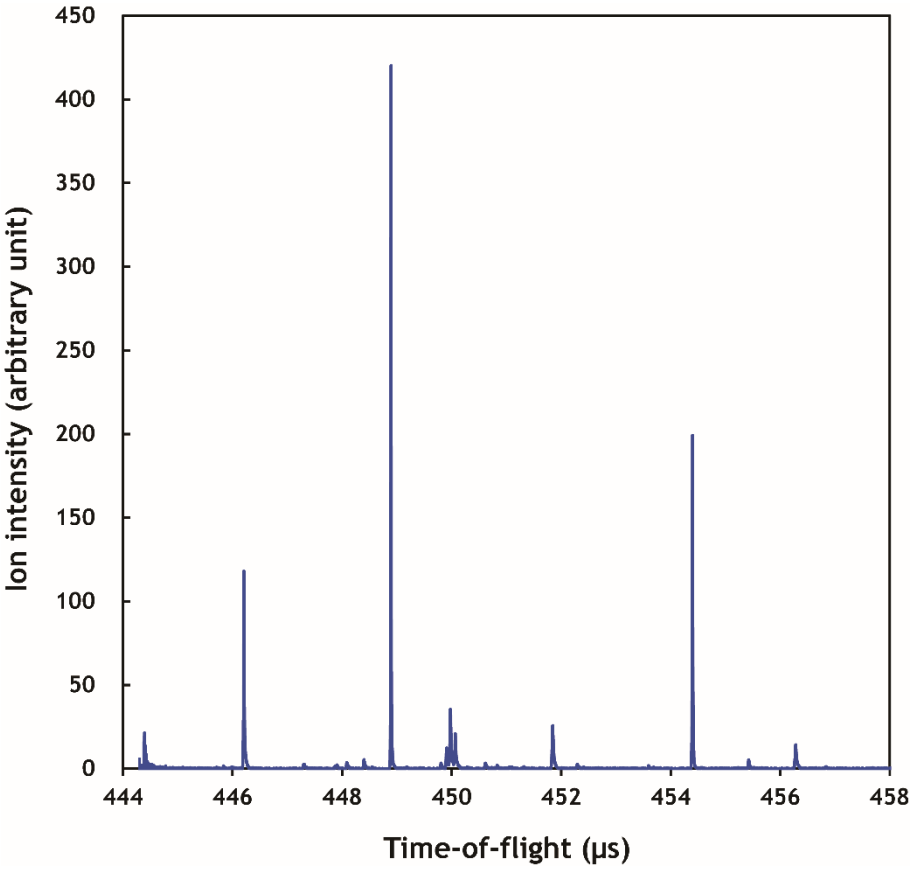

Figure 10. Multiturn TOF spectrum of PFTBA extracted from the multiturn trajectory.

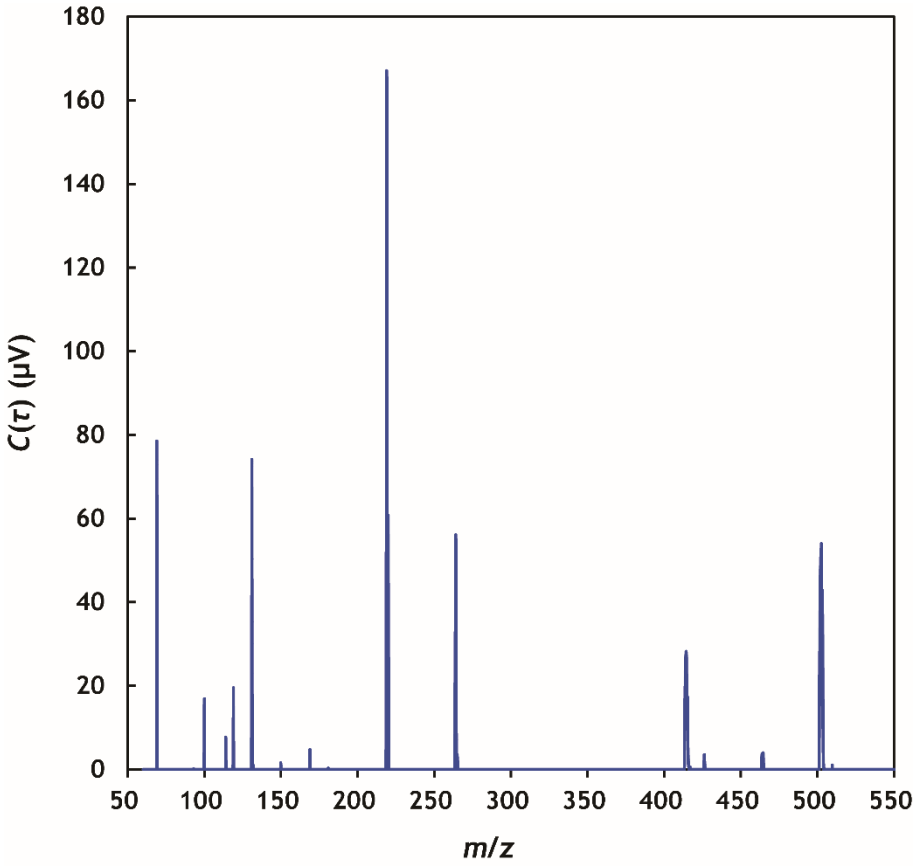

Figure 11. Convolved mass spectrum of PFTBA calculated from iCD spectrum. τ_{min}, τ_{max}, s_{τ}, t_0, Δt and V_{dis} were set at 5.76 μs, 17.28 μs, 0.0638 ns, 0.3781 τ, 384 ns, and 0 V respectively. The *m/z* (horizontal axis) is calculated from τ using internal mass references of *m/z* 68.9952 (CF_3^+) and 218.9856 ($C_4F_9^+$).

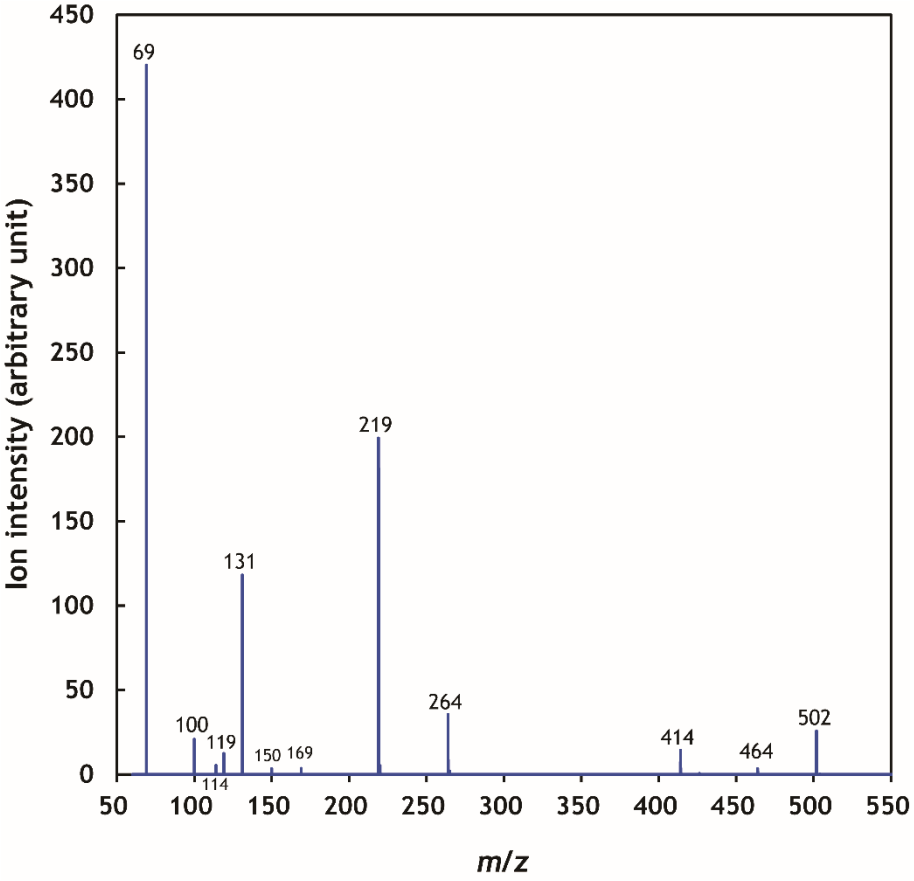

Figure 12. Extended convolved mass spectrum of PFTBA.

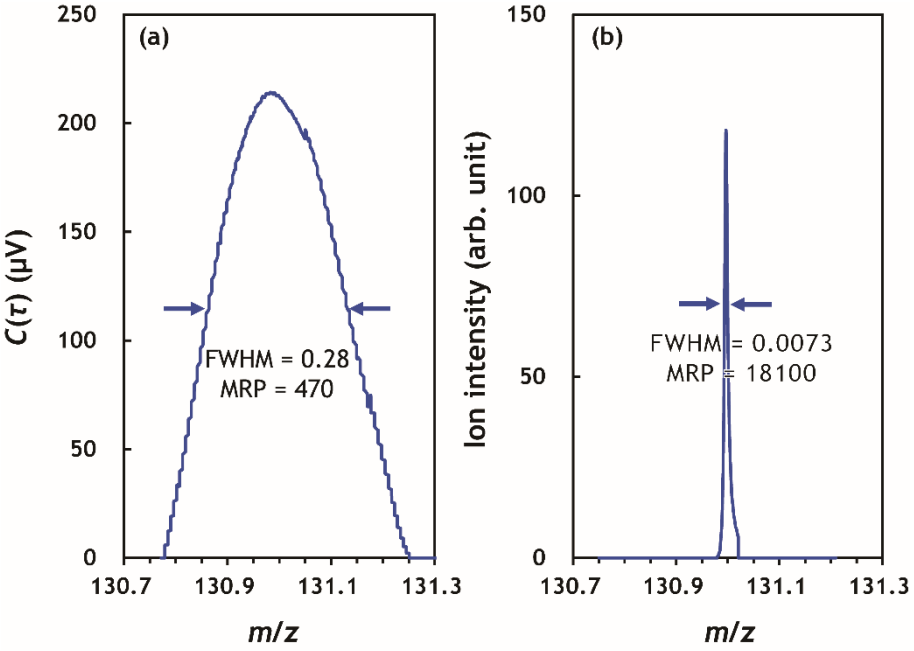

335

336 Figure 13. Peak shapes at *m/z* 130.9920 ($C_3F_5^+$) (a) from Figure 11, (b) from Figure 12.

337

Table 1. molecular formulas, exact masses, measured masses, mass differences (Δm), mass accuracies, number of laps, and mass resolution (MRP) of major peaks from PFTBA sample.

Molecular formula	Exact mass	Measured mass	Δm	Mass accuracy	Number of laps	MRP
			$\times 10^{-3}$	ppm		
CF_3	68.9952	68.9952	0.0	0	71	28200
C_2F_4	99.9936	99.9897	3.9	39	59	10800
$C_3F_4H_2$	113.9973	113.9926	4.7	42	55	9000
C_2F_5	118.9920	118.9876	4.4	37	54	10800
C_3F_5	130.9920	130.9897	2.4	18	51	18100
C_3F_7	168.9888	168.9797	9.1	54	45	7300
C_4F_9	218.9856	218.9856	0.0	0	40	20500
C_4F_9H	219.9935	219.9752	18.3	83	40	10300
C_5NF_{10}	263.9877	263.9807	7.1	27	36	9600
$C_5NF_{10}H$	264.9956	265.0001	−4.5	17	36	9800
C_8NF_{16}	413.9782	413.9701	8.1	20	29	8700
C_9NF_{18}	463.9750	463.9589	16.1	35	27	6900
C_9NF_{20}	501.9718	501.9678	4.0	8	26	8500